# PROCEEDINGS OF THE 3RD INTERNATIONAL SYMPOSIUM ON HEAT TRANSFER AND ENERGY CONSERVATION

Volume 2

Editors in Chief

Hua Ben , Guo Zengyuan and Ma Chongfang

SOUTH CHINA UNIVERSITY OF TECHNOLOGY PRESS

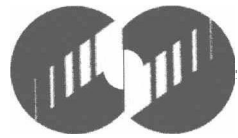

# 3rd ISHTEEC

## Proceedings of

## The International Symposium on Heat Transfer Enhancement and Energy Conservation

(Guangzhou, P. R. China January 12-15, 2004)

**Volume 2**

Editors in Chief
Hua Ben, Guo Zengyuan, Ma Chongfang

Editors
Zhu Dongsheng, Chen Qinglin, Gao Xuenong

South China University of Technology Press

Guangzhou

**图书在版编目（CIP）数据**

第三届国际传热强化与节能会议论文集（上、下册）/华贲，过增元，马重芳主编.—广州：华南理工大学出版社，2004.1

ISBN 7-5623-2019-5

Ⅰ.第… Ⅱ.①华… ②过… ③马… Ⅲ. 传热学 国际学术会议-文集-英文 Ⅳ.TK124-53

中国版本图书馆 CIP 数据核字（2003）第 120376 号

**总 发 行**：华南理工大学出版社（广州五山华南理工大学 17 号楼，邮编 510640）

发行部电话：020－87113487　87111048（传真）

**Eamil:scut202@scut.edu.cn　　http://www.scutpress.com**

**责任编辑**：胡　元　吴兆强

**印 刷 者**：广州大一印刷有限公司

**开　　本**：889×1194　1/16　**印张**: 98　**字数**: 3525 千

**版　　次**：2004 年 1 月第 1 版第 1 次印刷

**定　　价**：600.00 元（上、下册）

# EXPERIMENT OF HEAT TRANSFER ENHANCEMENT AND PERFORMANCE COMPARISON OF STRIP INSERTS IN HEAT TRANSFER TUBES

**Peng Deqi, Zhu Dongsheng, Dai Jianjun, Qian songwen**
Key Laboratory of Enhanced Heat Transfer and Energy Conservation, research Institute of Chemical Engineering, South China University of Technology, Guangzhou, 510640, China
Tel: 86-20-87114568, Fax: 86-20-87114140, Eamil:pengshuaike@163.com

## ABSTRACT

The paper introduces briefly many researches on heat transfer enhancement of strip inserts in heat transfer tube in the past. The heat transfer enhancement experiment of fin Strip inserts, flat steel strip and spiral iron twisted of tape inserts are conducted. Compared with other strip inserts, these strip inserts have performance of heat transfer enhancement and pressure drop increasing, therefore strip inserts will be reasonably chosen for application according to technical situation.

## INTRODUCTION

Many researchers had studied heat transfer enhancement of strip inserts in heat transfer tubes. Chen and Hsien researched forced convection heat transfer of laminar flow influenced by buoyancy with longitudinal installed strip inserts of rectangle section. Solanki *et al.* conducted experimental research and theoretical analyses of forced convection of laminar flow with core inserts of multi-angle section in heat transfer tubes. Chen and Hsien made a series of research on mixed convection of laminar flow with square core of rectangle longitudinal section inserted in horizontal heat transfer tubes, established AR (the ratio of longitudinal to horizontal section of rectangle strip), the radius ratio of inserts outfit circle to tubes and relative net effect of the ratio of heat transfer enhancement to pressure drop augmentation. Furthermore Hsien and Wen studied heat transfer of 3-dimensional steady laminar flow with different axial inserts in horizontal tube, resulted their performance such as heat transfer, secondary flow effect and nature, established Reynolds Number(*Re*), Grasof Number, *AR* and the radius ratio (*J*)of inserts outer circle to tube. The results matched experiments. In Fig.1 in horizontal tube Hsien&Huang tested heat transfer and pressure drop of laminar flow of crossed type strip with square (*AR*=1) and rectangle strip (*AR*>1). The inserts' heat transfer coefficient is 16 times more than smooth tube and the friction coefficient ( $f$ ) increases about 4.5 times; Saha& Dutta, Soha *et al.* found that the heat transfer performance of whole short strip inserts is much better than that of whole long strip inserts which is installed equal space in heat transfer tubes*(See Yongjoon Park, et al., 2000)*.

In Fig.2 The Technology Institute of Japan Waseda University and Key Laboratory of Enhancement Heat Transfer & Energy Conservation of Education Ministry in South China University of Technology (SCUT) developed the fin strip inserts, the performance of which is better than spiral strip inserts greatly. Its main parameters include fin length ($P_n$) and space of fin ($P_D$)*(see Xu Tianhua, 1984; Liu Zhenqiu, 1984; Qian Songwen, et al. 2003)*.

The experimental strip inserts could be denoted by code name according to strip inserts parameters. For instance, 2*D*~3*D* denotes the strip inserts whose parameter $P_n$ and $P_D$ were equal to 2 and 3 times diameter of inserts respectively. The Japanese experiment was conducted on the condition that the experimental medium was 90 turbine oil and the horizontal

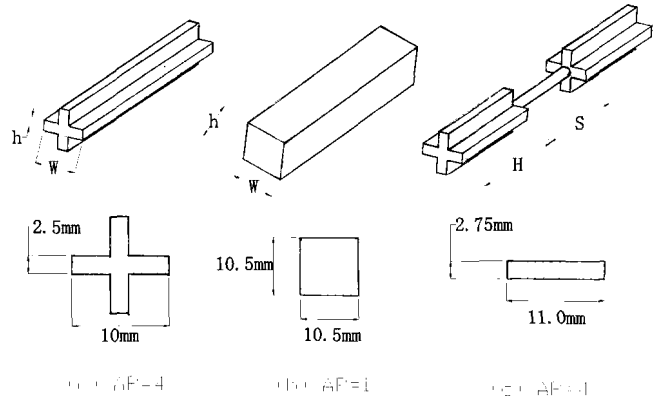


Fig.1 (a) Crossed section inserts .(b)Square section inserts (c) Rectangle section inserts (d) Installed discontinuously cross section inserts

installed tube outer-surface was cooled and its temperature kept constant, and then the experiments results were gotten as following:

(1) Heat transfer coefficient and pressure drop of tube inner were equal to 2~4 times and 2.5~2.6 times of its smooth tube respectively.

(2) When $P_n$ equaled to $P_D$, and the less $P_n$ was, the greater heat transfer coefficient of tube inner film and pressure drop was.

(3) To compared with 4*D*~4*D* inserts, if fin space was larger than fin length, the heat transfer coefficient of 4*D*~6*D* inserts was small about half, but pressure drop almost did not decrease.

(4) Strip inserts had ability to enhance heat transfer coefficient because there existed strong vortexes reaction in tube.

## 1 PERFORMANCE COMPARISON OF STRIP INSERTS

Furthermore we have conducted experiments of strip inserts with fin which is made up of copper, whose parameter is 4*D*~4*D*, 2*D* ~2*D* and 2*D*~1*D*, the experimental graph are shown in Fig.3 and 4. The results were gotten from Fig.3 and 4*(see Qian Songwen, et al. 2003;Wang Siqing,1993)*.

(1) Compared with smooth tube, heat transfer coefficient and pressure drop of strip inserts are 2.3~3.6 times greater and 3.7~9 times greater respectively.

(2) Compared with vertically installed 2*D*~2*D* strip inserts, heat transfer coefficient and pressure drop of horizontally installed 4*D*~4*D* strip inserts match of documents, in which the data difference is very little among many 4*D*~4*D* strip inserts. The experimental results are also shown in Fig.3 and 4 of flat steel strip and spiral iron twisted of tape ( *P/D*=8.2 P-pitch, *D*-diameter).

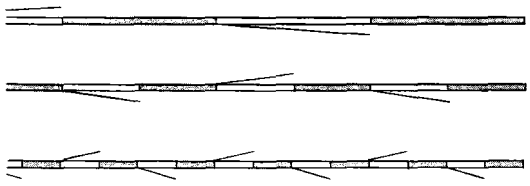

Fig.2 The experimental strip inserts of Japan Waseda University and SCUT

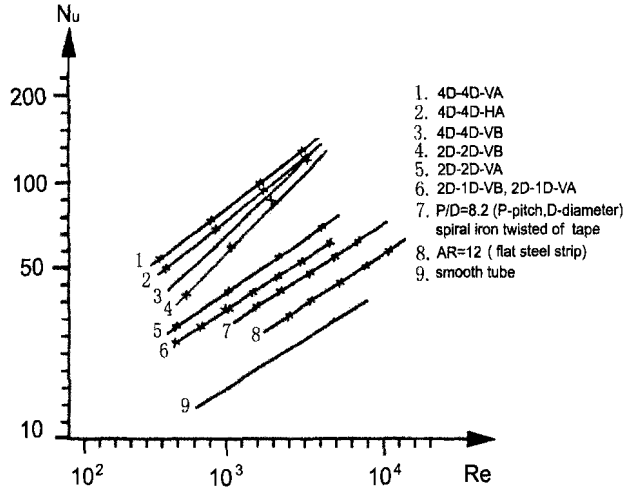


Fig.3 The heat transfer performance of strip inserts with fin and comparison with rectangle section inserts, twisted- tape inserts and smooth tube

Note:

A shows liquid flow direction is from fin root to fin tip,
B shows liquid flow direction is the opposition to A.

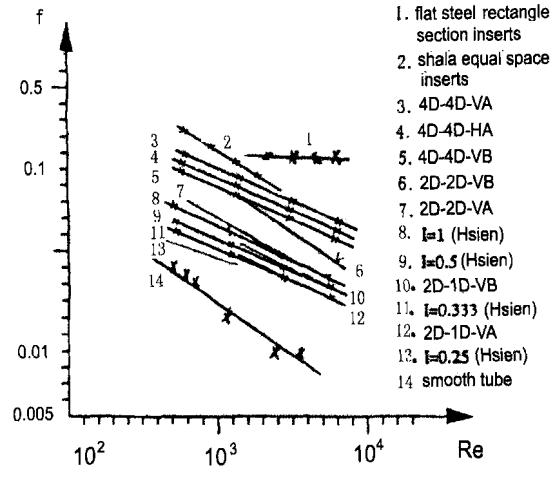


Fig.4 Comparison fiction coefficient of rectangle section inserts and finned strip inserts with Shala and Hsien & Wen inserts

Note:

A shows liquid flow direction is from fin root to fin tip,
B shows liquid flow direction is against A

To comparing with the experiment results of author and Shala with whose of Hsien and Wen's short whole strip inserts (the ratio $I$ of inserts length to tube length equal to 1, 0.5, 0.33 and 0.15 ), The results are gained and shown in Fig.3 and 4. Firstly, the performance of strip inserts with fin has been effected greatly by the liquid flow direction because of its liquid flow modes. Secondly, if liquid flow direction is from fin root to fin tip, the $Nu$ and $f$ are greater and the ratio $A/A_s$ and $P/P_s$ are small, but the results are absolutely reverse if liquid flow in opposition direction. Thirdly, when $P_n$ is equal to $P_D$, the performance of strip inserts with small fin is good.

But if $P_n$ is larger than $P_D$, the strip inserts with fin have good performance, for example when $Re$ equal to 1470, $A/A_s$ of $2D$~$1D$ strip inserts is 6 percent less than that of $2D$~$2D$ strip inserts, as $Re$ equal to 6000, $P/P_s$ of $2D$~$1D$ strip inserts is 20 percent less than that of $2D$~$2D$. But the performance of $2D$~$1D$ strip inserts is better than $2D$~$2D$ firstly because the fin space is shorter, then the fin number increase and swirl reaction is sharp. Secondly, energy consumption by friction is produced while liquid flows through the flat parts of strip inserts with fin. The energy consumption will decrease by shortening fin space.

In Fig.3 and 4 the results are gained that heat transfer enhancement of twist tape inserts are close to that of fin strip inserts, but its friction coefficient is largest. Heat transfer enhancement of $AR$ =12 flat inserts is lower and its friction coefficient is less than spiral iron twisted of tape and close to equal space strip inserts of Shala friction coefficient. Friction coefficient of Hsien and Wen short inserts has greatly decreased about 8%~58%, and also less than these of fin strip inserts, but its $Nu$ number decreased 2%~40%.

## 2 CONCLUSION

(1) Strip inserts have advantage of structure simplicity, processing facility and heat transfer enhancement, but its disadvantage is pressure drop increasing.
(2) Heat transfer performance of twist iron inserts approach to those of priority fin strip inserts, but pressure drop is rather great; flat steel inserts structure is very simple and its pressure drop is rather low, but the magnitude of enhancement of heat transfer is low; contrasted to whole strip inserts, pressure drop of short strip inserts is the lowest, but its $Nu$ number also reduce 8%~58%; the $Nu$ number of discontinue strip inserts is 15%~80% larger than this whole strip inserts, and at the same time the friction coefficient increases 1%~35%. In a word, strip inserts will be reasonable choose to apply according to technical situation.

## NOMENCLATURE

| | |
|---|---|
| $Nu$ | Nusselt Number |
| $Re$ | Renold Number |
| $f$ | fiction coefficient |

## ACKNOWLEDGEMENTS

Supported by the Excellent Young Teachers Program of M0E, China , Specialized Research Fund for the Doctoral Program of Higher Education, Guangdong Natural Science Foundation (No.011584), the Science & Technology Council Project Generalization Plan of Guangzhou City, and National Natural Science Foundation of China (No. 20346001).

## REFERENCES

Liu Zhenqiu, 1984, Research of Enhancement Freon horizontal condensation inside Tube Using New Inserts, *Master Dissertation,* South China University of Technology
Qian Songwen, Zhu Dongshen, Li Qingling, Yang Liming, 2003, Heat Transfer Enhancement Technology of Tube-Type Heat Exchanger, Chemical Industry Press
Wang Siqing, 1993, Heat Transfer Augmentation Theory and Experiment Research of Combined Radiation and Conductivity and Convection in High Temperature Silicon Carbon Tube Heat Exchanger Which is Made by a Equil-Pressure Method, *Master Dissertation,* South China University of Technology
Xu Tianhua, 1984, Research of Heat Transfer Enhancement of High Viscosity Liquid in Tube Using New Inserts, *Master Dissertation,* South China University of Technology
Yongjoon Park, Jaeenn Cha and Moohwan Kim, 2000, Heat Transfer Augmentation Characteristics of Various Inserts in a Heat Exchanger Tube, *Journal of Enhanced Heat Transfer*, 17:p23~33

Zhu Dongsheng, Tan Yingke, Anti-fouling, replacement and enhancement heat transfer insert. *China patent, no.95114893.1*
Zhu Dongsheng, Tan Yingke, 1990, Heat transfer of condensation augmentation of immiscible R113 and water in a horizontal tube, *Journal of Chemical Industry and Engineering (Chinese)*, no.3:p265-272
Zhu Dongsheng, Tong Zilong, Tan Yingke, 1998, An experimental study of porous surface tubes for pool boiling heat transfer enhancement of binary liquid mixture(Chinese), *Journal of Chemical Industry and Engineering (in English)*, (3), p355-360
Zhu Dongsheng and Wang Shengwei, 2002, Experimental investigation of contact resistance in adsorber of solar adsorption refrigeration, *Solar Energy*, Vol.73(3):p177-185
Tan Yingke, Zhu Dongsheng, 1992, An experimental study and simulation on adsorption heat pump cycle process, *Science et Technique du Froid*, no.1, p129-134

# HEAT TRANSFER AUGMENTATION FOR THE FLOW OF HIGHLY VISCOUS FLUIDS IN TUBES USING CROSS TRAPEZOID WAVE TAPE INSERTS

**He Lu, Zhu Dongsheng, Fan Zhonglei**
Key Laboratory of Enhanced Heat Transfer & Energy Conservation,
South China University of Technology, Guangzhou, 510640, China
Tel: 86-20-8711-4568, Email: cedshzhu@scut.edu.cn

## ABSTRACT

The development and heat transfer augmentation mechanism of a new type cross trapezoid wave tape (CTWT) insert was introduced. Experiments were conducted to evaluate the heat transfer, pressure drop and fouling characteristics of CTWT inserts for heating of polymer resin and heavy oil, respectively. 60%~120% increase in heat transfer efficiency was achieved, accompanied by a 100% increase in pressure drop over comparable empty tubes. It was also found that CTWT inserts could beneficially reduce the fouling of tubes. Correlations for over all heat transfer coefficient, Nusellt number and friction factor were derived from the experimental data.

## INTRODUCTION

The process of improving the performance of a heat transfer system is referred to as heat transfer augmentation, enhancement or intensification(*See Qian et al., 2003)*. Laminar flow heat transfer in tubes occurs in a wide variety of engineering application such as the heat transfer of highly viscous fluids*(See Zhu et al., 1990)*. Many augmentation techniques have been investigated to increase the low heat transfer coefficients in this type of flow*(See Hong et al., 1976)*. For shell and tube heat exchangers, the insertion in tubes of objects is one of the most important passive techniques *(See Zhu et al., 1998)*. The technique of enhanced heat transfer using inserts inside the tubes has been extensively investigated and widely applied since 1896, and several kinds of inserts such as twisted tapes, mesh inserts etc. have been developed.

A new type of insert-cross trapezoid wave tape (CTWT) insert*(See Zhu et al., 1995)* for augmenting heat transfer developed specially for highly viscous fluid was the subject of this paper. CTWT insert was developed on the basic of Cross Wave Insert tapes*(See Xu,1984)*. These types of inserts are different from the other inserts such as the twisted tape inserts and mesh inserts, which are shown comparing with CTWT inserts in Fig.1.

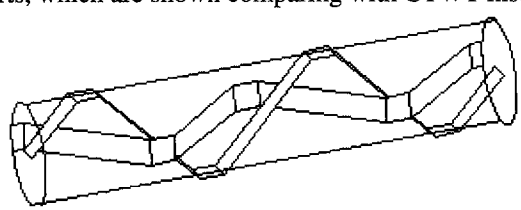

Cross Trapezoidal Wave Tapes insert (CTWT)

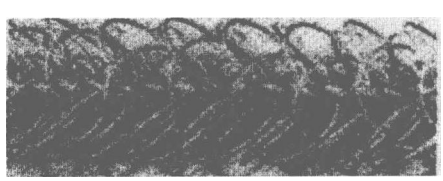

Twisted tape inserts

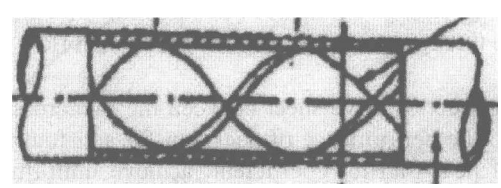

Mesh insert

Fig.1 Typical tube insert devices

Twisted tape inserts cause the flow to spiral along the tube length. Tong and Bergles(1996) found that the existence of the twisted tape reduced the heat transfer coefficient near the contact area between the twisted tape and tube wall.

This effect, named the thermal insulating effect, could degrade the heat transfer performance. The similar insulation effect is also reported by Agarwal(1996) using the name "cold-wall", which is most prominent in the case of viscous heat exchangers. The slow moving, high viscosity fluid layers near the wall tend to act as an insulator in the heat transfer process, which serves to impede an already poor heat transfer mechanism. Mesh inserts can disturb the entire velocity and temperature fields inside the tube*(See Wang et al., 2002)*, however, it suffers from high pressure drop and fouling problems*(See Megerlin et al., 1974)*.

For the case of tubes with CTWT inserts, this thermal insulation effect is reduced due to the special geometry structure of CTWT. The two cross trapezoid wave tapes induce turbulence, displacing and mixing fluid from the center of the tube to the wall of the tube. Thus the thermal insulating layer is destroyed. The heat transfer enhancement achieved by means of CTWT inserts is accompanied by an increase in pressure drop too, of course, however, the thermal and dydraulic performance is beneficially balanced. Another favorable advantage of CTWT inserts is that the fouling inside tubes is greatly reduced. It is noted that CTWT inserts are very inexpensive to fabricate and can be easily installed. They are one of the simplest of the various augmentation devices and can be fabricate in any moderately equipped workshop.

# 1 CROSS TRAPEZOID WAVE TAPE INSERT

## 1.1 Cross wave tape insert

Displaced promoters can be very beneficially used to augment lamina flow heat transfer of highly viscous fluid. In this paper, inserts were used to displace and mix the fluid in the center of the tube with that on the wall side, i.e., deflect the fluid to the wall to elevate the heat transfer.

The displacing and mixing process in a circular tube with cross wave tape insert was shown in Fig.2~3. According to the theory of relative activity, the fluid's flowing from left to right direction equals to the wave tape's moving from right to left direction. When wave tape move from right to left, slope I impacts a force upward on the fluid on the left, deflects the fluid to the wall side, and cause a circle flow around the slope. Similarly, slope II impacts a force downward. Suppose a tube is fixed with single wave tape, the fluid will thus form channel flow in the bow-shape channel beside the tape. To avoid channel flow, the insert consists of two cross wave tapes ( See Fig.3 ).

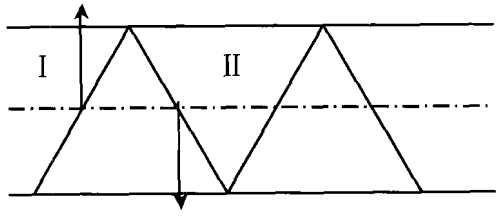


Fig.2 Illustration of working principle of Wave Tape

Fig.3 Cross wave tapes

## 1.2 Cross trapezoid wave tape insert

The slopes of cross wave tape inserts displace and mix fluid in the center and fluid on the tube wall constantly, and the center fluid is displaced quickly after moving to the tube wall. The contacting time between fluid and tube wall is too limited to obtain desirable performance. This disadvantage led to the development of CTWT insert. A flat or wave sheet is added between every two cross slopes. This series of stainless tapes are defined as Cross Trapezoidal Wave Tapes. The fluid moves from the center of the tube to the wall and fluid on the wall side flows to the center of the tube through the slopes, inducing turbulent flow in the boundary layer.

The flat sheet or wave sheet between the two crossing slopes prolongs the contacting time between fluid and tube wall. So the performance of heat transfer anti-fouling is better than other kinds of inserts. CTWT can increase the over all heat transfer coefficient, achieve uniform temperature profiles and reduce fouling of tubes. The cross trapezoidal wave tape insert consists of two cross trapezoidal wave tapes .The geometrical parameters are showed in Fig.4. The major geometrical parameters of the cross trapezoidal wave tape insert include the width of tape $b$, the angel of inclination of slope with tube axis $\alpha$ and the length of trapeziform hemline $e$. The cross trapezoidal wave tapes have a geometrical structure of periodicity of variety in axis direction. The whole cross trapezoidal wave tapes

are made up of several cross teeth, each of which is of one period width and identical geometrical structure.

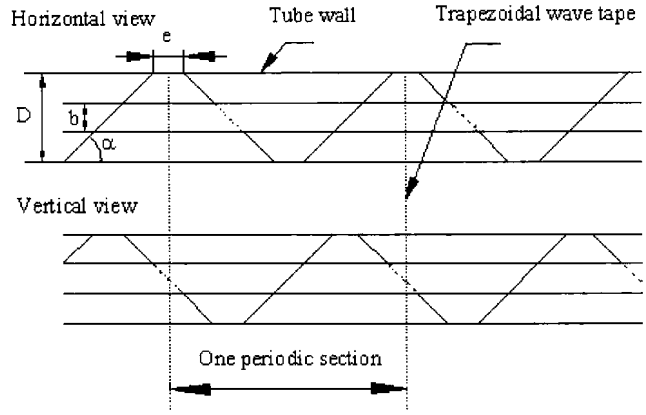


Fig.4 Illustration of CTWT inside a circular tube

## 2 EXPERIMENTAL PROCEDURE

In the present study, experiments of two highly viscous fluids polymer resin and heavy oil in tubes with CTWT inserts were carried out to investigate heat transfer, pressure drop and fouling characteristics, respectively.

The polymer resin was heated inside tubes in a tube-shell exchanger. The working pressure was 60 bar, and the flow rate was 16 L/min. Dry and saturated steam at a temperature of 120℃ was used as the heating medium. The viscosity of the polymer resin is 10 Pa· s (the viscosity of 25℃ water is 0.001Pa.s). Beside the extra high viscosity, another property of the polymer resin is that it is thermal sensitive. If the wall side temperature is too high (up to 120 ℃), the thermal sensitive material will react. The performance of tubes with CTWT inserts was compared to that of the tubes with twisted tape inserts and empty tubes based on variation of tube length.

Another fluid heavy oil was tested. The viscosity of heavy oil is very high, varies with the temperature. The relationship between the viscosity of heavy oil and temperature was shown in Table 1. The heavy oil was heated inside tubes in a tube-shell exchanger. Dry and saturated steam at a pressure of 0.5~0.85MPa was used as the heating medium in the heater. Renolds Number *Re* was range from 20 to 180,and Prantel number *Pr* was 1500. The performance of tubes with CTW inserts was compared to that of empty tubes based on variations of heavy oil flow rate and steam pressure. Due to the fact that heavy oil is very easy to foul in tubes after running for months, which always leads to the decreased heat transfer coefficients, the fouling of tubes with CTWT inserts was investigated in the present experiments after running for six months.

Table 1 The relationship between the viscosity of heavy oil and temperature

| Temperature | ℃ | 200 | 112 | 131 | 150 | 160 |
|---|---|---|---|---|---|---|
| Viscosity | E | 21.8 | 13.6 | 6.3 | 3 | 2(Engler unit) |

## 3 RESULTS AND DISCUSSIONS

### 3.1 The heating of high viscosity and thermal effective polymer resin

The performance of empty tube was tested. It was found that no matter how long the tube was, the highest temperature the polymer resin could reach was 50℃. It was also found that it was very difficult to heat the polymer resin and raise the temperature over 78℃ in tube with twisted tape inserts. The heat transfer results of heating of polymer resin were shown in Fig.5. The temperature of polymer resin inside tube with CTWT was higher than that of empty tube and twisted tape tube. At the length of 8m, the temperature of CTWT tube was 104℃, which was 54 ℃ higher than that of empty tube and 26℃ higher than that of twisted tape tube. The CTWT inserts presented a significant advantage for the heat transfer augmentation for the flow of high viscosity and thermal effective fluid.

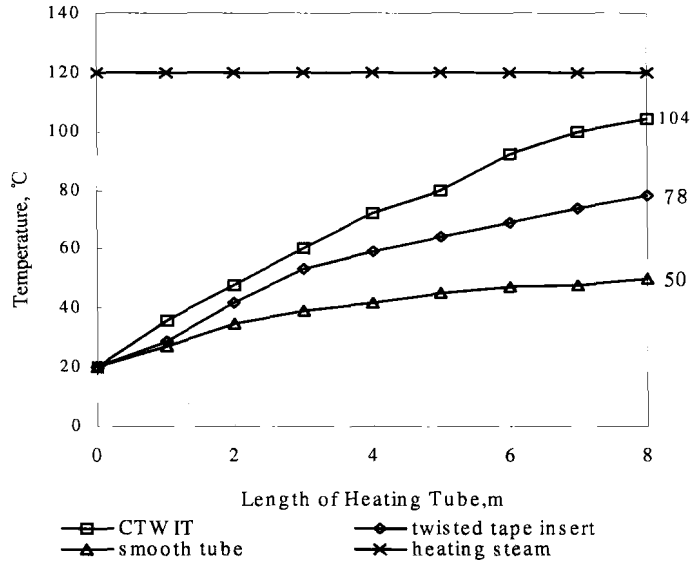


Fig.5 Heat transfer results of heating of polymer resin

### 3.2 The heating of heavy oil

Comparison of Pressure drop and heat flux for empty tube and CTWT tube was presented in Table 2. The flow rate of heavy oil was 17 t/h, and the pressure of steam is 0.8MPa.

Table 2 Comparison of data for empty tube with CTWT tube

| | Pressure Drop, MPa | Outlet Temperature, ℃ | Heat flux, W |
|---|---|---|---|
| Empty tube | 0.08 | 130 | 330 |
| CTWT tube | 0.15 | 154 | 523 |

It was found that 60% increase in the heat flux was achieve, and the out let temperature of CTWT tube was 24℃ higher than that of empty tube. At the same time, the heat transfer augmentation associated by a pressure drop penalty. The pressure drop was twice the empty tube value. However, the obvious improvement in heat transfer was much deserving than the corresponding increase in pressure drop.

Another heat transfer results were presented in Fig.6 for empty tube and CTWT tube at different steam pressure. The flow rate of heavy oil was 22t/h. The temperature difference obtained by CTWT tube was kept 30℃ higher than that of empty tube at the same steam pressure. It is found that tubes with CTWT inserts had much better operational performance than empty tube, and the outlet temperature of tube with CTWT arrived 154℃. It was concluded that tube with CTWT inserts could obtain significant heat transfer augmentation over the comparable empty tube.

The heat transfer results for flow of heavy oil in CTWT tube and empty tube after running for six months was shown in Fig.7. The heavy oil inlet temperature was 100℃ and the steam pressure was 0.7MPa. Compared with data presented in Fig.6, under the same condition of flow rate of 22t/h and steam pressure of 0.7MPa, the temperature difference of CTWT tube was found to decease 1 to 2℃. It was due to the fouling inside tube after months of operation. However, the temperature difference of empty tube was found to decease average 10℃, which was 5~10times the CTWT tube values. It was concluded that the fouling was greatly reduced in the tube with CTWT inserts.

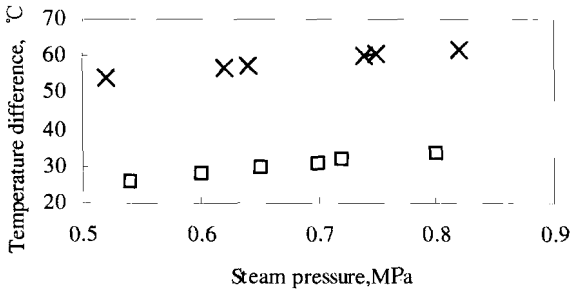


× CTWT □ Empty tube

Fig.6 Heat transfer results for heating of heavy oil

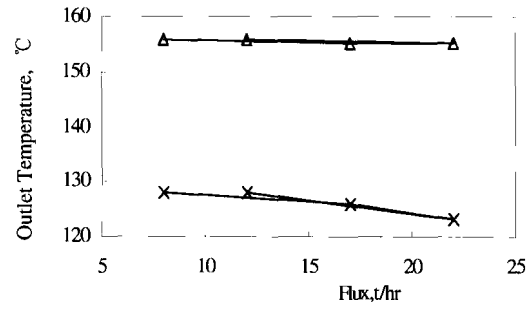


△ CTWT × Empty tube

Fig.7 Heat transfer results for flow of heavy oil after running for six months

In addition, it was found that the fluid outlet temperature was kept about 150℃, almost independent of flow rate and heat flux. It showed that the sensitivity of film heat transfer coefficient inside the tube to flow rate was not reduced, but more applicable for the operation in which the flow rate varied greatly.

The regressive correlation of over all heat transfer coefficient was developed using the experimental data of CTWT insert:

$$K = C \cdot Re^{0.998} \tag{1}$$

The Nusellt number correlation read:

$$Nu = 0.07996 Re^{0.9419} \tag{2}$$

Base on the same data, a correlation for the friction factor was developed.

$$f = 2.7908 Re^{-0.3758} \tag{3}$$

## 4 CONCLUSION

A new type of cross trapezoid wave tape (CTWT) insert developed specially for the flow of high viscosity fluid was introduced in this paper. Experiments of two highly viscous fluids polymer resin and heavy oil in tubes with CTWT inserts were carried out respectively to investigate heat transfer, pressure drop and fouling characteristics. 60%~120% increase in heat transfer efficiency was achieved. It is found that tubes with CTWT inserts had better performance than twisted tape tube and empty tube. At the same time, the heat transfer augmentation associated by a pressure drop penalty. The pressure drop was twice the empty tube value. However, the obvious improvement in heat transfer was much deserving than the corresponding increase in pressure drop. It was also concluded that tube with CTWT inserts could obtain significant anti-fouling effect over the comparable empty tube. Correlations for the heat transfer coefficient, Nusellt number and friction factor were derived from the experimental data.

## NOMENCLATURE

| | | | |
|---|---|---|---|
| $D$ | tube diameter m | $Nu$ | Nusellt number |
| $b$ | tape width m | $Re$ | Renolds Number |
| $e$ | length of trapeziform hemline m | $Pr$ | Prantel number |
| $\alpha$ | the angle of inclination of slope with tube axis deg | $f$ | friction factor |
| $K$ | overall heat transfer coefficient W/(m$^2$·℃) | | |


## ACKNOWLEDGEMENTS

Supported by the Excellent Young Teachers Program of M0E, China , Specialized Research Fund for the Doctoral Program of Higher Education, Guangdong Natural Science Foundation (No.011584), the Science & Technology Council Project Generalization Plan of Guangzhou City, and National Natural Science Foundation of China (No. 20346001).

## REFERENCES


Agarwal S.K., Rajarao M.R., 1996, Heat transfer augmentation for the flow of a viscous liquid in circular tubes using twisted tape inserts, Int. J. Heat Mass Transfer, Vol.39:p3547-3557

Hong S.W., Bergles A.E., 1976, Augmentation of Laminar flow Heat transfer in Tubes By means of Twisted-tape Inserts, Journal of Heat Transfer, Vol.5:p251-256

Megerlin F.E., Murphy R.W., Bergles A.E., 1974, Augmentation of heat transfer in tubes by use of mesh and brush inserts, Journal of Heat Transfer, Vol.5:p145-151

Qian S.W., Zhu D.S., Li Q.L., Yang L.M., 2003, Heat transfer enhancement technology of tube-type heat exchanger, *Chemical Industry Press*

Tong W., Bergles A.E., Jensen M.K., 1996, Critical heat flux and pressure drop of subcooled flow boiling in small-diameter tubes with twisted-tape inserts, *Journal of Enhanced Heat Transfer*, Vol.3(2):p95-108

Wang L., Sunden B., 2002, Performance comparison of some inserts, *Int. Comm. Heat Mass Transfer*, Vol.29:p45-56

Xu T.H., 1984, Tube inserts for enhancement of Liquid Heat Transfer, *Ph.D. thesis, The Key Laboratory of Enhanced Heat Transfer & Energy Conservation, South China University of Technology*, China

Zhu D.S., Tan Y.K, 1990, Heat transfer of condensation augmentation of immiscible R113 and water in a horizontal tube, *Journal of Chemical Industry and Engineering (Chinese)*, No.3:p265-27

Zhu D.S., Tan Y.K., 1995, Anti-fouling, replacement and enhancement heat transfer insert, *China Patent: No.95114893.1*

Zhu D.S., Tong Z.L., Tan Y.K, 1998, An experimental study of porous surface tubes for pool boiling heat transfer enhancement of binary liquid mixture(Chinese), *Journal of Chemical Industry and Engineering*, Vol.3:p355-360

# FLOW AND HEAT TRANSFER IN LEC GROWTH OF GALLIUM ARSENIDE

**Li Mingwei, Zeng Danling**
Institute of Power Engineering, Chongqing University, Chongqing, 400044, China
Tel: 86-23-65415008, Fax: 86-23-65102473, Email: mwlizao@yahoo.com

## ABSTRACT

Numerical simulations for momentum and heat transfer for a 2 inch diameter LEC growth of single-crystal GaAs with an axial magnetic field was conducted using the finite-element method. Convective and conductive heat transfers, radiative heat transfer between diffuse surfaces and the Navier-Stokes equations for both melt and encapsulant and electric current stream function equations for melt and crystal are all combined and solved simultaneously. The effect of the thickness of encapsulant, the imposed magnetic field strength as well as the crystal rotation rate on the flow and heat transfer were investigated.

## INTRODUCTION

Gallium arsenide is usually grown in liquid encapsulated Czochraski [LEC] puller. To grow high quality GaAs crystal, an ideal thermal circumstance is required. The thermal circumstance is associated with furnace structure and the operate conditions, such as the thickness of encapsultant, crystal and crucible rotation, as well as the imposed magnetic field. To understand the characteristics of the momentum and heat transfer in a LEC growth of GaAs, some numerical simulations have been performed by neglecting the melt flow*(See F.Dupret, 1990; P.D.Thomas, 1989; J.Fainbery, 1997)*. Actually, the melt flow is one of the important factors influencing the crystal quality, and it is well known that the crystal and crucible rotation, as well as the thickness of the encapsulant have an impact on the melt flow and melt/crystal interface shape. The effect of rotation rate of the crystal and crucible on the fluid flow, instability, heat transfer and interface shape was emphasized*(See V.I.Pplezhaev, 2001)*. Numerical simulation of the flow and heat transfer in the melt and encapsulant and heat transfer in the crystal for LEC growth of GaAs with a steady, uniform, axial magnetic field has done by Sabhapathy A constant crucible sidewall temperature is imposed, the melt/crystal interface and melt/encapsulant interface are assumed to be flat and un-deformable. Their numerical results show that the flow in the bulk of the melt is suppressed by the magnetic field*(See P.Sabhapathy, 1990)*.

In the present paper, a set of numerical simulations on momentum and heat transfer for a 2-inch diameter Liquid Encapsulant Czochralski growth of single-crystal GaAs were performed. The effect of the thickness of encapsulant, the imposed axial magnetic field and the rotation rate of crystal on the flow and temperature field and interface shape was discussed.

## 1 MODEL FORMULATION

### 1.1 Physical model and basic assumptions

Schematic diagram adopted in the present analyses is shown in Fig.1, in which the GaAs melt/encapsulant interface shape is calculated by solving the Young-Laplace equation. The following assumptions were introduced in the model.

(1) The system is in a pseudo-steady state and is axisymmetric.(2) The flow is laminar and both the GaAs melt and the boron oxide encapsulant are incompressible. (3) Thermophysical properties of the melt are assumed to be constant except for the temperature dependencies of surface tension and the dynamic viscosity of boron oxide. (4) No subcooling occurs at the melt/crystal interface and the interface shape

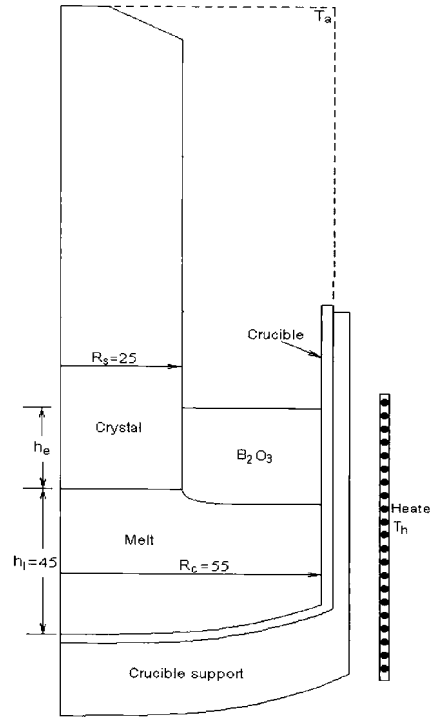


Fig.1 Schematic diagram of a LEC growth of GaAs

coincides with the melting temperature isotherm. (5) The magnetic Reynolds number is so small that the effect of the induced magnetic field on the applied field can be neglected.

## 1.2 Mathematical model

### 1.2.1 Governing equations

Under the above assumptions, the general governing equations for flow and temperature field are given as follows. In the melt and encapsulant:

$$\nabla \cdot v_i = 0, \tag{1}$$

$$\rho_i v_i \cdot \nabla v_i = -\nabla p_i - \nabla \cdot \tau_i + \rho_i g \beta (T_i - T_m) e_z + (J \times B) \tag{2}$$

$$\rho_i c_{pi} v_i \cdot \nabla T_i = \lambda_i \nabla \cdot \nabla T_i, \tag{3}$$

In the crystal:

$$\rho_s c_{ps} V_s e_z \cdot \nabla T_s = \lambda_s \nabla \cdot (\nabla T_s) \tag{4}$$

In the other solid materials:

$$\nabla \cdot (\nabla T_j) = 0 \tag{5}$$

where $T$, $v$, $p$, and $\tau$ are the temperature, velocity vector, pressure and stress tensor, respectively. $T_m$ is the melting temperature, . $\rho$ the density, $\lambda$the. thermal conductivity, $\beta$ the thermal expansion coefficient, $g$ the gravitational acceleration constant, $c_p$ the heat capacity, $V_s$ the crystal pulling rate, respectively. Subscripts $i$, $s$, and $j$ indicate GaAs melt($i$=l), $B_2O_3$ encapsulant($i$=e), crystal and other materials, respectively. Vector $e_z$ is a unit vector parallel to the z axis. Product ($J \times B$) represents the Lorentz force due to the imposed magnetic field, in which $J$ is the electric current density and $B$ is strength of the magnetic field. The electric current density $J$ are calculated by introducing the electric current stream function $\psi_j$ which is determined by the following equation:

$$\frac{\partial}{\partial z}\left(\frac{\xi_l}{\xi}\frac{1}{r}\frac{\partial \psi_j}{\partial z}\right) + \frac{\partial}{\partial r}\left(\frac{\xi_l}{\xi}\frac{1}{r}\frac{\partial \psi_j}{\partial r}\right) = B_z \frac{\partial w}{\partial z} + B_r r \frac{\partial}{\partial z}\left(\frac{w}{r}\right) \tag{6}$$

Where $\psi_j$ is the electric current stream function defined by:

$$J_z = -\frac{\xi_l B_0}{r}\frac{\partial \psi_j}{\partial r} \tag{7}$$

$$J_r = -\frac{\xi_l B_0}{r}\frac{\partial \psi_j}{\partial z} \tag{8}$$

where $\xi$ is the electrical conductivity and $B_0$ is the magnetic field strength. The above equations is valid both in the melt ($\xi$=$\xi_l$) and in the crystal ($\xi$=$\xi_s$).

### 1.2.2 Boundary conditions for the temperature field

At the melt/encapsulant interface:

$$-\lambda_l n \cdot \nabla T_l = -\lambda_e n \cdot \nabla T_e + q_{rad,l} \tag{9a}$$

At the encapsulant free surface:

$$-\lambda_e n \cdot \nabla T_e = q_{rad,e} \tag{9b}$$

At the melt/crystal interface:

$$\lambda_l n \cdot \nabla T_l - \lambda_s n \cdot \nabla T_s = \rho_s V_s \Delta H_s n \cdot e_z \tag{9c}$$

$$T_l = T_s = T_m \tag{9d}$$

At the encapsulated crystal side:

$$-\lambda_s n \cdot \nabla T_s = -\lambda_e n \cdot \nabla T_e + q_{rad,s} \tag{9e}$$

At the encapsulated crucible side:

$$-\lambda_j n \cdot \nabla T_j = -\lambda_e n \cdot \nabla T_e + q_{rad,j} \tag{9f}$$

At the exposed crystal side and top:

$$-\lambda_s n \cdot \nabla T_s = q_{rad,s} \tag{9g}$$

At the other exposed surfaces:

$$-\lambda_j n \cdot \nabla T_j = q_{rad,j} \tag{9h}$$

In these equations, $q_{rad,i}$ is the net radiative heat flux per unit area on the surfaces, and is given by

$$q_{rad,i} = \varepsilon_i \sigma_B \left[ T_i^4 - \left( \sum_j A_j \varepsilon_j T_j^4 G_{ji} \right) \Big/ \left( A_i \varepsilon_i \right) \right] \tag{10}$$

where $G_{ji}$ is Gebhart's absorption factor, which is the fraction of emission from surface $A_j$ to $A_i$ and absorbed, $G_{ji}$ as well as the view factors between each surface element in the furnace are calculated using our code and $\Delta H_s$ is the latent heat of fusion, $n$ the unit normal vector of the interface element and $\varepsilon$ the emissivity.

1.2.3 Boundary conditions for the flow field and electric current stream function

At the side wall and the bottom of the crucible:

$$u_l = v_l = 0, \quad w_l = r\omega_c, \quad \psi_j = 0. \tag{11a-d}$$

At the encapsulated side wall of the crucible:

$$u_e = v_e = 0, \quad w_e = r\omega_c. \tag{11e-g}$$

At the melt/encapsulant interface:

$$n \cdot v_l = 0, \quad n \cdot v_e = 0, \psi_j = 0 \tag{11h-j}$$

$$\tau_l : nt - \tau_e : nt = \gamma_T \nabla T_l \cdot t \tag{11k}$$

$$t \cdot v_l - t \cdot v_e = 0 \tag{11l}$$

$$\tau_l : n\mathrm{e}_\theta - \tau_e : n\mathrm{e}_\theta = \gamma_T \nabla T_l \cdot \mathrm{e}_\theta \tag{11m}$$

$$\mathrm{e}_\theta \cdot v_l - \mathrm{e}_\theta \cdot v_e = 0 \tag{11n}$$

At the encapsulant surface

$$n \cdot v_e = 0 \tag{11o}$$

$$\tau_e : nt = \gamma_T \nabla T_e \cdot t \tag{11p}$$

$$\tau_e : n\boldsymbol{e}_\theta = \gamma_T \nabla T_e \cdot \boldsymbol{e}_\theta \tag{11q}$$

At the melt/crystal interface:

$$u_l = v_l = 0, \quad w_l = r\omega_s \tag{11r-t}$$

At the encapsulated surface of crystal:

$$u_e = v_e = 0, \quad w_e = r\omega_s, \quad \psi_j = 0 \tag{11u-x}$$

At the other crystal surface:

$$\psi_j = 0 \tag{11y}$$

At the axis:

$$\psi_j = 0 \tag{11z}$$

Where $u$, $v$, and $w$ are the radial, axial and the azimuthal components of velocity, $\omega_s$ and $\omega_c$ are the angular rotation rates of the crystal and crucible, respectively. Symbol $t$ and $\mathrm{e}_\theta$ are the unit tangential and azimuthal vectors of each interface element, respectively. The melt/crystal interface shape is determined so that Eq.(9d) is satisfied, i.e., the interface coincides with the melting-point isotherm.

## 1.3 Numerical procedure

By applying Galerkin finite element method, the system gives a set of algebraic equations. In the present work, the diameter and length of the crystal and the heater temperature were given. The crystal pull rate was determined as one of the unknown variables, together with velocities, pressures, temperatures, electric current stream function and the melt/crystal interface coordinates, by simultaneously solving the set of nonlinear algebraic equations using Newton-Raphson method. The radiative heat exchange in the semi-transparent boric oxide layer is calculated by using the band-energy method*(See F.Dupret, 1990)*.

## 2 RESULTS

To make the comparison of the results valid, the pulling rates were maintained at around 5 mm/hr within ±1% for all cases by adjusting the heater temperature.

### 2.1 Effect of encapsulant thickness

Fig.2 and Fig.3 show the isotherms (left) and contours of stream function (right) under two different thickness $h_e$ of encapsulant with a fixed magnetic field strength and crystal and crucible rotation rate. A strong flow cell driven by Marangoni force combined buoyancy force occupies the main region of melt. A weaker anti o'clock cell appears under the tri-point when $h_e$=1.0 cm. Flow in the encapsulant is significant distinct for various encapsulant thickness, mult-cell flow may be observed with increase of thickness $h_e$. The M-type interface shape will be influenced slightly by encapsulant thickness as seen in Fig.8.

### 2.2 Effect of magnetic field strength

The effect of the magnetic field strength on the flow and heat transfer for a fixed thickness of encapsulant, crystal and crucible rotation rate is shown in Fig.3, Fig.4 and Fig.8. The thin Ekman layer induced by crucible rotation is observed at the bottom of the crucible (See Fig.4) for a weaker magnetic field strength, with increasing the axial magnetic field strength, the flow in the melt is suppressed effectively (See Fig.5). When increasing the dimensionless Hartmann number from 44 to 155 the maximum velocity $V_{max}$ and the average velocity $V_{av}$ in the melt decrease from $V_{max}$=1.24 cm/s and $V_{av}$=0.4 cm/s at $Ha$=44 to $V_{max}$=0.31 cm/s and $V_{av}$=0.097 cm/s at $H_a$=155; meanwhile, the deflection of the interface increases from 1.03 mm to 3.77 mm as shown in Fig.8. Here the average velocity $V_{av}$ is defined as follow: $V_{av} = \Sigma\left(\sqrt{u_i^2 + v_i^2}\right)/N$, where $N$ represents the total number of the nodes in the melt.

### 2.3 Effect of crystal and crucible rotation

Crystal rotation has a remarkable effect on the flow pattern and heat transfer. A new cell appears beneath the melt/crystal interface near closely the periphery and it will get larger with increasing rotation rate of maximum velocity $V_{max}$ and the average velocity $V_{av}$ in the melt almost do not change with the change of crystal rotation rate $\omega_s$. Due to more effective heat transfer resulting from the forced convective cell driven by crystal rotation, the

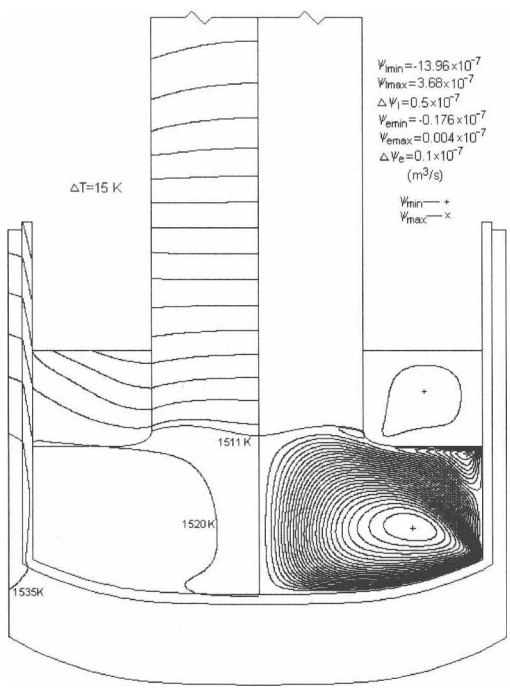


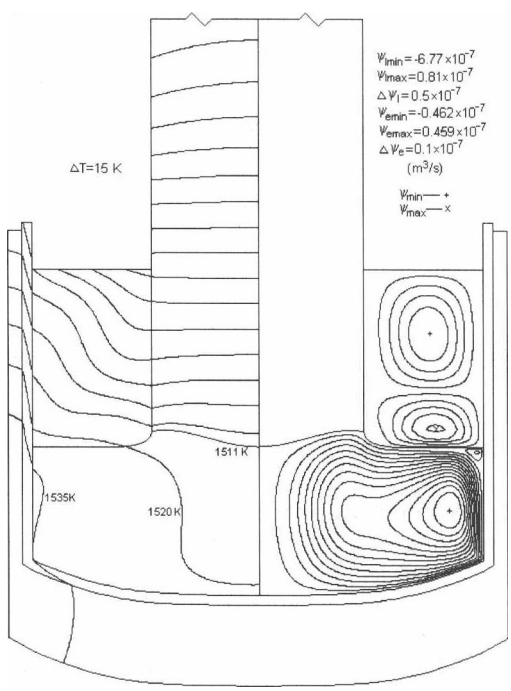


Isotherms and contours of stream function with $H_a$ = 111, $\omega_s$ = 6 rpm, $\omega_c$ = 16 rpm

Fig.2 (left) $h_e$ = 1.0 cm Fig.3 (right) $h_e$ = 1.0 cm